© Department of Physics, FEE CTU in Prague, 2023

A PRESSURE BASED COMPRESSIBLE SOLVER FOR ELECTRIC ARC-PLASMA SIMULATION

S. Coseru[a,*], S. Tanguy[b], P. Freton[a,b], JJ. Gonzalez[a,b]

[a] *IMFT, UMR CNRS 5502, Université de Toulouse, 2 Allée du Professeur Camille Soula, 31400 Toulouse, France*

[b] *LAPLACE, UMR CNRS 5213, Université Paul Sabatier Toulouse 3, 118 route de Narbonne, 31062 Toulouse Cedex France*

* sergiu.coseru@laplace.univ-tlse.fr

Abstract. The electric arc discharge in a liquid medium is used in several applications such as the sterilization of the liquid by UV radiation, the fracturing of rocks by shock wave, the circuit breakers in oil bath or the forming of mechanical parts. Thus, describing the physics of the arc in a liquid and in particular its interaction with a liquid interface is an important issue to better characterize this type of configuration. However, such a challenging task requires to couple high-fidelity solver for compressible two-phase flows with liquid phase change and a plasma solver to describe the plasma and its interaction with the bubble. To study this type of medium, we use a compressible formulation of the fluid equations. For this purpose, a pressure based solver has been developed for the computation of the energy conservation equation. Moreover, our numerical model uses the immersed boundary method to simulate the solid electrodes. The numerical model is briefly described in this paper and the first results of the electric arc discharge in steam water are presented. To our knowledge this pressure based model has never been used to describe plasmas and electric arc discharge.

Keywords: electric arc, plasma, compressible, pressure-based.

1. Introduction

Numerical Simulations is a powerful tool which can be complementary to experiments for a better understanding of the plasma behavior in water. The electric arc in liquid water creates a centimeter-sized bubble of plasma and acoustic waves. The simulation based on commercial CFD solvers, as Fluent, can hardly simulate the interaction between, the acoustic waves, the plasma and two-phase flows. When dealing with simulation of compressible flows one have to be careful for the numerical stability at different Mach numbers [1]. We can achieve an asymptotically preserving solution through compressible semi-implicit solvers based on pressure [2]. The compressible entropic two-phase flow solver, developed in [3] seem adapted for the problem at hand. In particular, the formulation of the energy conservation equation based on the pressure variable is suitable to describe acoustic waves, which are described implicitly, while being well suited to describe two-phase flows. The objective is verify the aptitude of these solvers to correctly simulate plasma flows. This solver is integrated in the home made code DIVA [4] in which specific plasma solvers have also been integrated. Moreover, this compressible solver is coupled to an immersed boundary method to account for complex geometry, as the solid surface of the electrodes [5]. We describe in this paper some preliminary results obtained with our solver on single-phase flows with acoustic waves in presence of an electrical arc between two electrodes in a water gas medium. Future developments on the extension of our solver to compressible two-phase flows with liquid-vapor phase change are also discussed.

2. Hypotheses

☐ 2 Dimensional and axisymmetric hypothesis.

☐ Local Thermodynamical Equilibrium (LTE) for plasma

☐ Laminar flow

☐ No sheath description

☐ No numerical resolution inside the solid material.

☐ Only the water gas phase is considered in the modeling

3. Theory

We present in this section the physical model for compressible flows which has been coupled to the Immersed Boundary Method developed in [5]. The formulation of the energy equation is pressure based, and equations of state accounting for a gas and plasma state enable to compute the temperature field from the density and pressure fields obtained by solving conservation equations. The model uses the equations of conservation of mass, momentum and energy described here:

The mass equation for the change of density ρ:

$$\frac{\partial \rho}{\partial t} + \nabla \cdot (\rho \vec{u}) = 0. \tag{1}$$

The momentum equation to compute the velocity field $\vec{u}$:

$$\frac{D\vec{u}}{Dt} + \frac{\nabla p}{\rho} = \frac{1}{\rho}\nabla \cdot \boldsymbol{\tau} + \vec{g}. \qquad (2)$$

The volume forces coefficient is $\vec{g}$ in this particular case it is the gravitational acceleration. The viscosity tensor is $\boldsymbol{\tau}$ and the viscosity coefficient is μ:

$$\boldsymbol{\tau} = \mu(\nabla\vec{u} + \nabla\vec{u}^T) - \frac{2}{3}\mu\nabla \cdot \vec{u}\mathbf{I}. \qquad (3)$$

The pressure based energy equation for the pressure p, proposed in [3], can be expressed as:

$$\frac{Dp}{Dt} = c^2\frac{D\rho}{Dt} + \left.\frac{\partial p}{\partial s}\right|_\rho \frac{Ds}{Dt}. \qquad (4)$$

Here s is the entropy $\frac{D}{Dt}$ is the material derivative, c is the speed of sound. The left hand side representing the evolution of pressure. On the right hand side the first term is associated to acoustic waves, and the second one is associated to heat transfer. The term responsible for the acoustic propagation $c^2\frac{D\rho}{Dt}$ is solved implicitly. Instead of the time step $\mathrm{d}t = \frac{\mathrm{d}x}{u+c}$, numerical stability is ensured with $\mathrm{d}t = \frac{\mathrm{d}x}{u}$ where u is the speed of the fluid. This is an advantage in the plasma medium in which the sound speed can reach very large values, such as $10\,\mathrm{km/s}$ which would involve very small values of the time step with classical compressible solver. This pressure based solver allows stability gain of the solver while being able to describe acoustic waves. To solve these equations, we use classical second order finite volume schemes for the spatial discretization, except the convection terms $(\overrightarrow{u} \cdot \nabla)(\overrightarrow{u})$ which are solved using a fifth-order WENO-Z (weighted essentially non-oscillatory) method [6].

To close our system of equations, an equation of state is required. Although, the present work is focused on electrical arc in a single-phase flow, cubic equations of state have been implemented since they allow to model the thermodynamics state, both in a gas phase and a liquid phase, as shown in [3]. This will be an asset for coming works on electrical arc in a liquid pool. For higher temperatures when dissociation of the molecules happen, data tables are implemented in our solver for a more accurate description of the density, temperature and pressure in the plasma state. These data tables are obtained using a solver based on minimization of energy.

An electric current with a linear profile is imposed on half of the radius of the upper electrode and the lower electrode is at a reference potential taken to be zero. The boundary conditions on the electric field are imposed on the electrodes using the Immersed Boundary Method and the lateral conditions impose an electrical insulation $\vec{n} \cdot \nabla V = 0$ with $\vec{n}$ being the normal vector, here V is the electric potential. Solving the following equation gives the electric potential field which is coupled to the conductivity coefficient σ

$$\nabla \cdot (\sigma\nabla V) = 0. \qquad (5)$$

It is noteworthy that the voltage drop deduced by the model only represents the column contribution as the sheaths description is not included in our model. From the electric potential field computation, the electric current density field $\vec{J}$ is computed in the fluid and the corresponding heat release due to Joule effect $\frac{\vec{J}\vec{J}}{\sigma}$ measured in $\frac{\mathrm{W}}{\mathrm{m}^3}$ is included as a source term in the pressure equation $\frac{Ds}{Dt}$. The magnetic field induced by the electric current is also taken into account. This magnetic field is calculated using a simplification, assuming that the electric current is parallel to the symmetry axis of the cylindrical electrodes. This allows to write simply the magnetic field as:

$$\vec{B} = \frac{\mu_0}{R}\int_0^R j_z\, r\,\mathrm{d}r, \qquad (6)$$

where $\vec{B}(R)$ is the magnetic field, R is the radius coordinate of the point in axisymmetric coordinate, and j_z is the electric current component parallel to the axis of symmetry. The effect of this magnetic field will be to deflect the charged fluid flow between the electrodes. At the same time a constant current is assumed inside the volume of the electrodes meaning $j_z(r)$ is a constant, from which the magnetic field created around the electrodes is deduced.

In the plasma phase the thermodynamical properties of plasma, depending on the local temperature and pressure, are extracted from tables. The sound speed is computed with a simple perfect gas law $c = \sqrt{\gamma\frac{p}{\rho}} = \sqrt{\frac{c_p}{c_v}\frac{p}{\rho}}$, γ being the heat capacity ratio, which is consistent with experimental data.

Radiation is included using the net emission coefficient ϵ. The term $4\pi\epsilon$ is added to the change of entropy term $\frac{Ds}{Dt}$.

4. Results

4.1. Acoustics

A first benchmark is proposed in order to illustrate the capability of our compressible solver to describe the interaction between an acoustic wave and a solid complex geometry imposed with an Immersed Boundary method. It consists in a long tube of air through which an acoustic wave of an arbitrary pressure amplitude propagates. Here the amplitude of the pressure is taken at $100\,\mathrm{Pa}$. The section of the tube is reduced at the middle of the domain, which generates a reflected acoustic wave and a transmitted acoustic wave. This behavior is highlighted in Figure 1, where we can visualize the propagation of the acoustic wave at different times: $t = 0\,\mathrm{ms}$, $t = 0.75\,\mathrm{ms}$, $t = 1.9\,\mathrm{ms}$, and the formation of a reflected wave after the impact of the incident wave with the section reduction. A theoretical prediction of the amplitudes of both waves can be obtained from a linear acoustic theory. The reflection and transmission coefficients, which depend on the section ratio, have been plotted in Figure 2

(a)

(b)

(c)
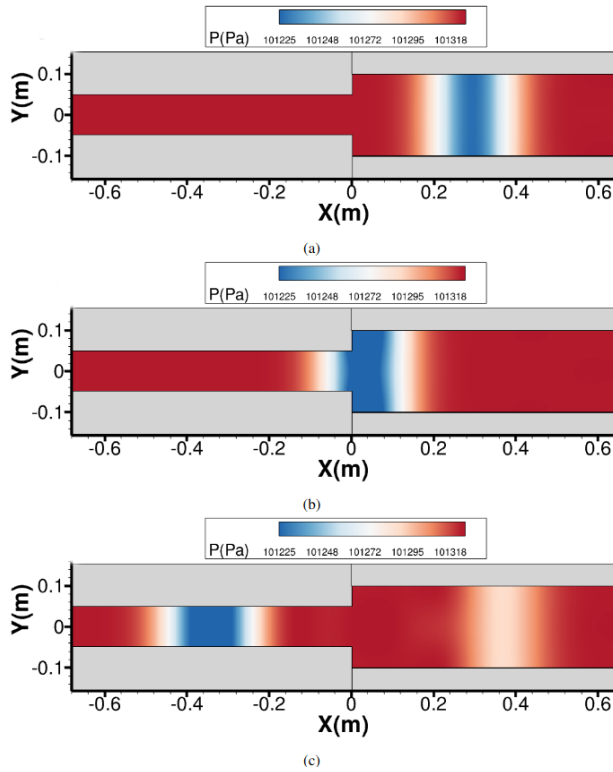
Figure 1. Acoustic wave propagation in a tube. The wave is propagated from right to left with a change of section in the middle. After the incident wave impacts at the section reduction, it splits into 2 waves: transmitted wave going to the left and the reflected wave going to the right. The figure times are: for (a),$t = 0\,ms$, for (b) $t = 0.75\,ms$, for (c) $t = 1.9\,ms$

where x-axis represents different section ratios. This demonstrates a good agreement between the theory and our numerical predictions.
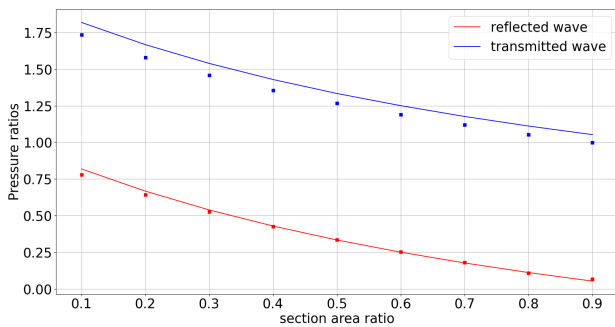
Figure 2. Comparisons between numerical simulation and linear acoustic theory on the transmission and reflection coefficients. The point represent numerical simulation for different section ratios of tubes and the continuous graph represents the theoretical solution.

4.2. Plasma

We present in this subsection, some preliminary results obtained with the overall solver which couples a solver for compressible flow with an immersed boundary method and a plasma solver to describe the electric arc. The simulation is performed on an axisymmetric grid.
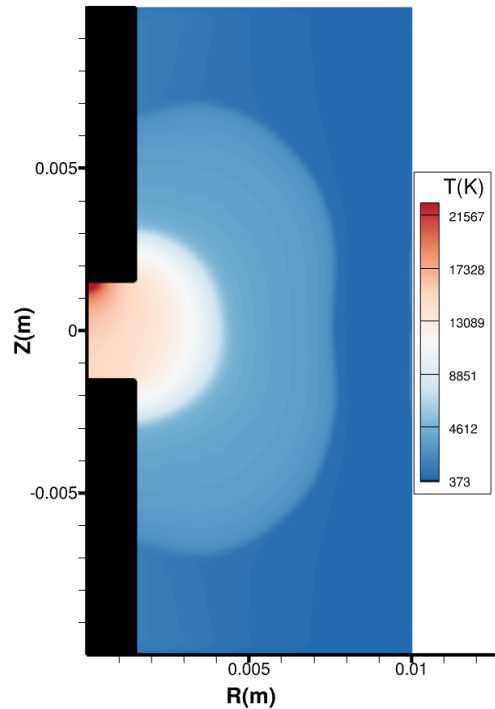
Figure 3. The temperature field between the black electrodes taken 90 microseconds after the start of the simulation.

The mesh is regular with a 40 micrometers cell size which corresponds to a mesh containing 256×512 cells. The gas used is water vapour at an initial pressure slightly below atmospheric pressure 95800 Pa. The computational domain is a cylinder of 1 cm radius and
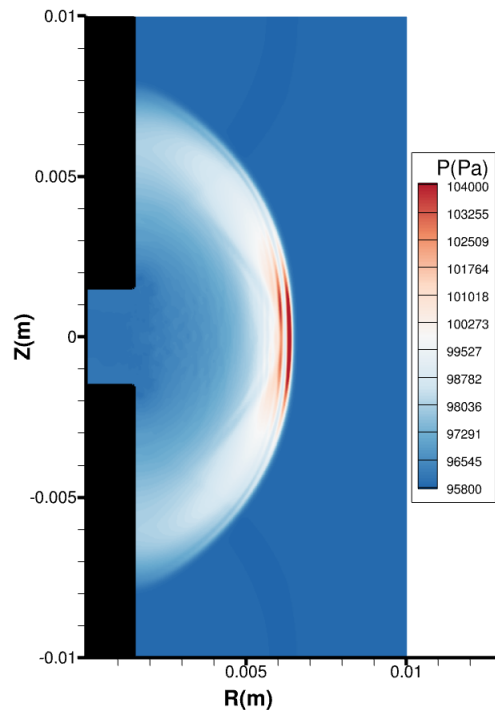
Figure 4. Pressure wave traveling away from the electrodes 6 microseconds after the start of the simulation
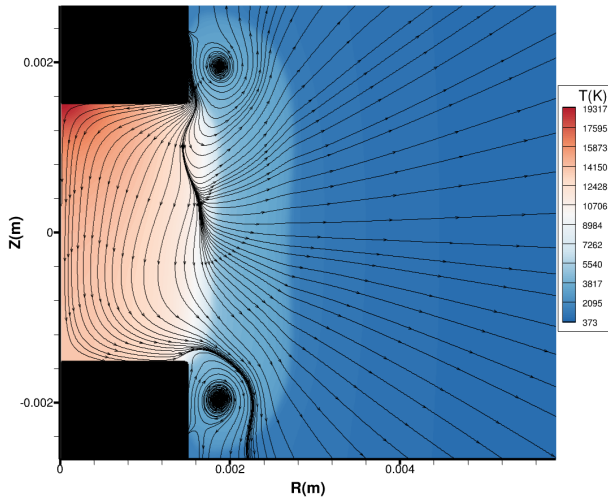
Figure 5. The velocity streamlines 20 microseconds after the start of the simulation. The streamlines are superimposed on the temperature field.

Figure 6. Electric potential field between the electrodes represented with the color-map. The streamlines represent the passage of electric current.

2 cm height, and the electrodes are 3 mm apart and have a radius of 1.5 mm. Neumann boundary conditions are imposed on the temperature $\vec{n} \cdot \nabla T = 0$ on the electrodes. The initial conditions are an uniform temperature everywhere except between the electrodes where a hot canal of 7000 K is initialized to allow the plasma formation at the beginning of the simulation. We impose an electric current with a total intensity at an arbitrary value of 100 A constant in time. In Figure 3, we can visualize, the temperature field and the expansion of the plasma with a maximum temperature around 20000 K in the vicinity of the electrode. The solver has shown its ability to describe the pressure wave in the test case in Figure 4. The arc ignition is not represented in our model as the plasma is initialized with a hot canal (7000 K) so the shock wave in Figure 4 is only due to initial temperature difference between the hot canal and the surrounding cold gas. The velocity streamlines are presented in Figure 5. Velocity between both electrodes has a typical magnitude of 40 m.s^{-1}. The electric potential and the electric current streamlines are presented in Figure 6. We can observe the current density distribution in the plasma column. We can also observe that the total voltage obtained is around 7 Volts. This value corresponds to the column voltage as sheath description is not taken into account.

5. Conclusion

In this paper, we have briefly described the numerical solver that we are currently developing for the interaction between an electric arc discharging in a liquid pool and a plasma bubble. It combines a solver for compressible flow with an Immersed Boundary method to account for complex geometry in our computational domain and a plasma solver for electric arcs. Our solver enables to capture the generation of acoustic waves and their interactions with the plasma
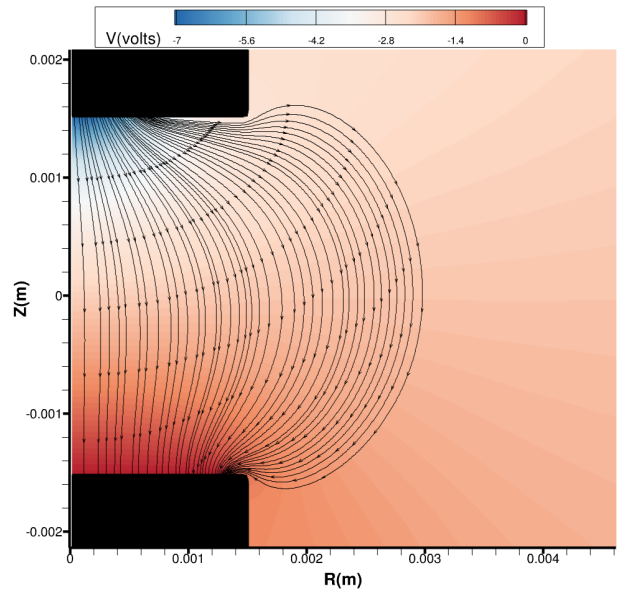
medium. As the present work only considers a single phase flow, future works will focus on its coupling with a two-phase flow solver accounting for liquid-vapor phase change, in order to predict the formation and the growth of a plasma bubble in a liquid pool.

References

[1] F. Xiao, R. Akoh, and S. Ii. Unified formulation for compressible and incompressible flows by using multi-integrated moments ii: Multi-dimensional version for compressible and incompressible flows. *Journal of Computational Physics*, 213(1):31–56, 2006. doi:10.1016/j.jcp.2005.08.002.

[2] N. Kwatra, J. Su, J. T. Grétarsson, and R. Fedkiw. A method for avoiding the acoustic time step restriction in compressible flow. *Journal of Computational Physics*, 228(11):4146–4161, 2009. doi:10.1016/j.jcp.2009.02.027.

[3] A. Urbano, M. Bibal, and S. Tanguy. A semi implicit compressible solver for two-phase flows of real fluids. *Journal of Computational Physics*, 456:111034, 2022. doi:10.1016/j.jcp.2022.111034.

[4] A. Dalmon, M. Lepilliez, S. Tanguy, et al. Direct numerical simulation of a bubble motion in a spherical tank under external forces and microgravity conditions. *Journal of Fluid Mechanics*, 849:467–497, 2018. doi:10.1017/jfm.2018.389.

[5] M. Lepilliez, E. R. Popescu, F. Gibou, and S. Tanguy. On two-phase flow solvers in irregular domains with contact line. *Journal of Computational Physics*, 321:1217–1251, 2016. doi:10.1016/j.jcp.2016.06.013.

[6] R. Borges, M. Carmona, B. Costa, and W. S. Don. An improved weighted essentially non-oscillatory scheme for hyperbolic conservation laws. *Journal of Computational Physics*, 227(6):3191–3211, 2008. doi:10.1016/j.jcp.2007.11.038.